Modularized and Reconfigurable Wireless Power Transfer: Architecture, Modeling and Analysis

Huan Zhang[1], Chengbin Ma[1], Ming Liu*[2]
[1]University of Michigan-Shanghai Jiao Tong University Joint Institute, Shanghai, China
[2]School of Electronic Information and Electrical Engineering, Shanghai Jiao Tong University, Shanghai, China
hzhang_93@sjtu.edu.cn, chbma@sjtu.edu.cn, mingliu@sjtu.edu.cn

***Abstract*—Megahertz (MHz) wireless power transfer (WPT) system is becoming a research trend because of its flexible spatial freedom. However, the high frequency circuit components limit the power level of MHz WPT system. Meanwhile, the actual application scenarios are changeable, so a single system design cannot meet the needs of multiple applications. In this paper, a design concept of modularized and reconfigurable MHz WPT is proposed to improve the system power level and design flexibility. With this method, the system requirements (power, efficiency and transfer distance) can be easily satisfied by the combination of modules. The design concept will be detailed explained through the analysis of the system architecture and the mathematical model. Finally, the influence of proximity effect and mutual inductance divergence achieves briefly analysis according to the simulation and test. And the modularized design concept is basically verified by the power and efficiency test results of four different combinations of UMs.**

***Index Terms*—modularized and reconfigurable, megahertz, wireless power transfer (WPT), proximity effect.**

I. Introduction

Wireless power transfer (WPT) system operating at MHz is becoming a research trend in the mid-range transfer for middle amount of power because of its features of flexible spatial freedom and circuit compactness [1], [2] My paper. However, the conventional switching devices will have higher power loss in MHz operation frequency because of the non-negligible parasitic parameters, e.g. gate charge and output charge. And the improved switching components with more ideal characteristics, i.e. higher switch speed and smaller parasitic parameters, like GaN MOSFET, can only endure lower voltage level because of the material limit. Thus, MHz WPT system tends to have lower power level compared with the kHz one.

Many researches have been discussed in order to improve the power level and efficiency of MHz WPT system. Class EF topology is utilized in MHz WPT system to reduce the peak voltage on the power components while maintaining high efficiency ZVS working condition [3]. Furthermore, the push-pull class E structure also achieves wide discussion to solve the power level and efficiency problems [4]. On the other hand, lower switching losses and higher power level can also be obtained at MHz system when using GaN material MOSFET in Class D topology design. Although the above researches make full use of the power components, system power level is still limited by single power components parameters. Meanwhile, in actual application scenarios, the charged device generally has different sizes requirements and spatial locations (charging distance), load characteristics, power requirements, etc. Thus, a single system design is very difficult to meet the needs of multiple applications.

In order to break through the power limitation of MHz WPT and apply the designed system in different applications, a design concept of modularized and reconfigurable wireless power transfer is detailed discussed in this paper. Based on this concept, different WPT applications can be achieved through the combinations (numbers and connection methods) of wireless power transfer unit modules (UM), as shown in Fig.1. Each physical application is consist of pre-designed several transmitting unit modules (TxUM) and receiving unit modules (RxUM). Each TxUM or RxUM has the same circuit structure and parameters. According to the different system requirements (power level and transmitting distance), the system will be achieved by corresponding combination of modules. And the input/output voltage relationship can be adjusted by the modules' connection method. Furthermore, the reconfigurable and modularized WPT system will not only provides design flexibility, but also reduce the cost and time period in design and production procedures. Meanwhile, the system will have higher reliability and maintainability because of the modularized design.

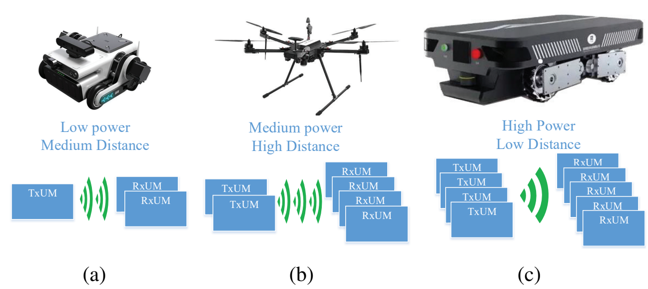

Fig. 1. Different WPT applications and power transfer features. a) Commercial motion robot b) Multi-rotor drone c) Industrial motion robot.

The remainder of this paper is organized as follows: Section II firstly analyzes and compares different modularized system architectures from the perspectives of scalability and reliability. Based on the chosen architecture, a specific composition of each module will be introduced. In Section III, the mathematical model of modularized system will be derived to provide the theory foundation of the system. And influence

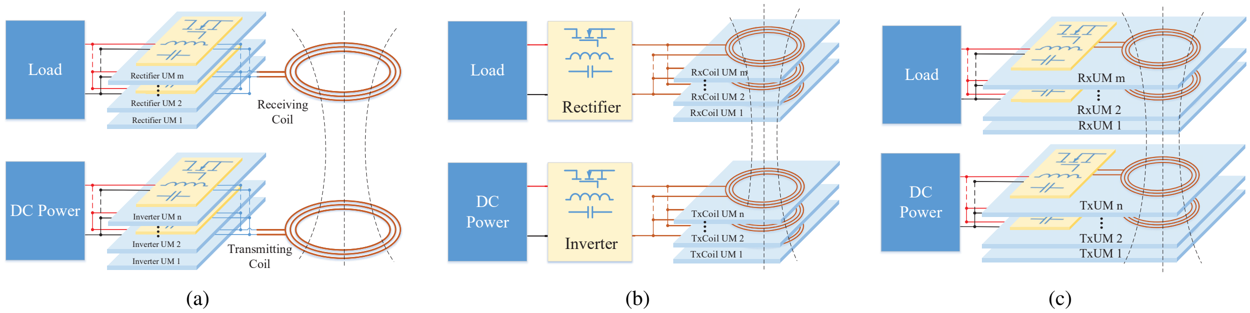

Fig. 2. Different WPT modularized architecture. a) Converter modularized architecture b) Coil modularized architecture. c) Function modularized architecture.

of the module connection methods will also be discussed in this part. The experimental results of the modularized WPT will be presented in Section IV. Finally, Section V concludes this paper.

II. Architecture Analysis of Modularized and Reconfigurable WPT System

There are mainly three kinds of modularized WPT system architecture, as shown in Fig.2. Fig.2(a) represents the converter modularized architecture. Through the using of several power converter modules (inverter UM and rectifier UM in the figure), the system can transfer more power at the same circuit component limit. In the existing research, this kind of modularized design has been widely discussed [5]. And the common full-bridge and push-pull structure have the same design philosophy [4]. With this architecture, the design power target can be easily realized by adjusting the modules number and the system may achieve high reliability. However, the power scalability of this architecture will be limited by the coupling coil. As the power level increases, the coil current will increase accordingly. Since the loss of the coil is proportional to the square of the current, the heating problem of the coupling coil will become particularly serious and thus decrease the system efficiency. In order to overcome this problem, coupling coil with better working performance should be redesigned, which will extend the design time period and increase cost.

Fig.2(b) illustrates the WPT system with coupling coil modularized architecture. The coupling structure is consist of several transmitting coil UM (TxCoil UM) and receiving coil UM (RxCoil UM). This multi-coil structure can significantly improve the transfer efficiency and distance of the coupling mechanism. However, its scalability is limited by the design capacity of the power converter. When the power needs to be increased, the power converter needs to be renewed to meet the demand; if the design capacity of the initial power converter has sufficient margins, the device utilization will be low which decreases the converter efficiency.

Fig.2(c) provides a function modularized architecture. Each module has independent power converter and coupling coil, which means it has complete power transmitting/receiving function, namely the function module. This architecture retains the scalability and reliability of converter modularized design. And the stacking of coils in each module can also reduce coil loss and increase transmission distance. The similar architecture in transmitting side has received some discussions in recent kHz system design [6]. However, due to the necessity of ferrite and litz wire using, the kHz system can not achieve module reconfiguration through coils direct stacking. As a contrast, the coils working at MHz will no longer need ferrite to enhance the coupling and can be produced by printed circuit board (PCB). Furthermore, since the thickness of PCB coil can be very small, the coupling condition of different RxUM and TxUM will be very similar with each other, which enable the modules achieve high consistency during system operation. Therefore, the combination of MHz operation frequency and function modules architecture will become the best candidate in achieving modularized and reconfigurable WPT system.

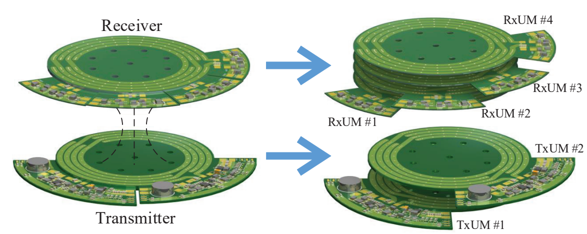

Fig. 3. 3D diagram of modularized and reconfigurable WPT system

As shown in Fig. 3, WPT transmitter (receiver) is consist of several TxUMs (RxUMs) stacking. Each module contains a MHz converter and PCB coils. In order to realize the flexible reconfiguration of the WPT modules, each converter (including power circuit, driver and power supply) should be stable and independent. The structure which can achieve these design target is shown in Fig. 4. The power circuit can be achieved by different kind topology, e.g. half-bridge and class E. The low power buck provides the power to MHz driver and other components independently. And the key to achieve the modules independence is the MHz isolator which isolates the outside driving signal and maintains signal synchronization meanwhile.

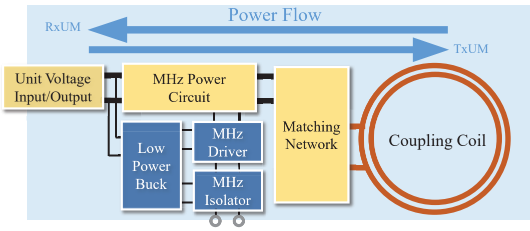

Fig. 4. The converter structure for function modules architecture design.

III. Derivation of Mathematical Model of the Modularized and Reconfigurable WPT System

Suppose the number of TxUM and RxUM is n and m in the modularized and reconfigurable WPT system respectively, the coupling condition is shown in Fig. 5. The coupling is complex and matrix will help to analyze the relationship.

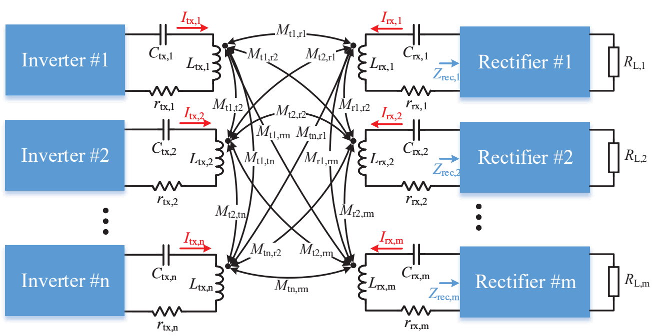

Fig. 5. Coupling condition of modularized and reconfigurable WPT System

A. Receiver Analysis

Suppose the voltage induced on receiving coil $\#i$ is equivalent to $U_{rx,i}$. Then, matrix equation can be derived:

$$\mathbf{U_{rx}} = j\omega\mathbf{M_{tr}}\mathbf{I_{tx}} + j\omega\mathbf{M_{rr}}\mathbf{I_{rx}} \tag{1}$$

in which $\mathbf{U_{rx}}$, $\mathbf{I_{tx}}$ and $\mathbf{I_{rx}}$ represents the vector of induced voltage and current in receiving and transmitting coil. $\mathbf{M_{tr}}$ represents the coupling between transmitting and receiving modules. $\mathbf{M_{rr}}$ represents the coupling inside the receiving modules, namely the receiver cross-coupling matrix.

$$\begin{aligned}\mathbf{M_{tr}} &= \begin{bmatrix} M_{\mathrm{t1,r1}} & M_{\mathrm{t2,r1}} & \cdots & M_{\mathrm{tn,r1}} \\ M_{\mathrm{t1,r2}} & M_{\mathrm{t2,r2}} & \cdots & M_{\mathrm{tn,r2}} \\ \vdots & \vdots & \ddots & \vdots \\ M_{\mathrm{t1,rm}} & M_{\mathrm{t2,rm}} & \cdots & M_{\mathrm{tn,rm}} \end{bmatrix}_{m\times n} \\ \mathbf{M_{rr}} &= \begin{bmatrix} 0 & M_{\mathrm{r1,r2}} & \cdots & M_{\mathrm{r1,rm}} \\ M_{\mathrm{r2,r1}} & 0 & \cdots & \vdots \\ \vdots & \vdots & \ddots & M_{\mathrm{rm,r(n-1)}} \\ M_{\mathrm{rm,r1}} & \cdots & M_{\mathrm{rm,r(n-1)}} & 0 \end{bmatrix}\end{aligned} . \tag{2}$$

Assuming $\#i$ rectifier input impedance equal to $Z_{\mathrm{rec,i}} = R_{\mathrm{rec,i}} + jX_{\mathrm{rec,i}}$ and receiving coil resonance impedance equal to $Z_{\mathrm{rxcom,i}} = r_{\mathrm{rx,i}} + j\omega L_{\mathrm{rx,i}} + \frac{1}{j\omega C_{\mathrm{rx,i}}}$, the total receiver impedance will be calculated as:

$$Z_{\mathrm{R,i}} = Z_{\mathrm{rxcom,i}} + Z_{\mathrm{rec,i}}. \tag{3}$$

Based on Ohm's Theorem, the induced voltage also satisfy the matrix equation:

$$\mathbf{U_{rx}} = -\mathbf{Z_R}\mathbf{I_{rx}}. \tag{4}$$

Take (4) into (1), an equation reflected current relationship will be derived:

$$-\mathbf{Z_R}\mathbf{I_{rx}} - j\omega\mathbf{M_{rr}}\mathbf{I_{rx}} = j\omega\mathbf{M_{tr}}\mathbf{I_{tx}} \tag{5}$$

Thanks to the high consistency provided by thin PCB coils, each receiving module may have very similar working condition. Thus, the receiver current can be assumed to be identical, e.g. $\dot{I}_{\mathrm{rx,1}} = \dot{I}_{\mathrm{rx,2}} = \cdots \dot{I}_{\mathrm{rx,m}}$. Thus, the influence of cross-coupling matrix $\mathbf{M_{rr}}$ in (5) can be equivalent to a variation in receiver reactance:

$$Z_{\mathrm{Rnew,i}} = Z_{\mathrm{R,i}} + j\omega \sum_{k=1}^{k=m,k\neq i} M_{\mathrm{ri,rk}} \tag{6}$$

When the receiving modules achieve fully resonance, the resonance capacitor can be calculated as follow:

$$C_{\mathrm{rx,i}} = \frac{1}{\omega\left(\omega L_{\mathrm{rx,i}} + X_{\mathrm{rec,i}} + \omega \sum\limits_{k=1}^{k=m,k\neq i} M_{\mathrm{ri,rk}}\right)}. \tag{7}$$

The equation (5) can then be simplified to:

$$\mathbf{I_{rx}} = -j\omega(\mathbf{Z_{R,new}})^{-1}\mathbf{M_{tr}}\mathbf{I_{tx}} \tag{8}$$

B. Transmitters Analysis

Similar with the receiving ones, the induced voltage on transmitting side can be expressed as:

$$\begin{aligned}\mathbf{U_{tx}} &= \omega^2\mathbf{M_{tr}}^{\mathrm{T}}(\mathbf{Z_{R,new}})^{-1}\mathbf{M_{tr}}\mathbf{I_{tx}} + j\omega\mathbf{M_{tt}}\mathbf{I_{tx}} \\ &= \mathbf{Z_{ref}}\mathbf{I_{tx}} + j\omega\mathbf{M_{tt}}\mathbf{I_{tx}}.\end{aligned} \tag{9}$$

It is obvious that $j\omega\mathbf{M_{tt}}\mathbf{I_{tx}}$ is equivalent to the reactance increase in transmitting coil which can be compensated by resonance capacitor in transmitting side $C_{\mathrm{tx,i}}$. The previous item in (9) represents the influence of the receiver on transmitter, which can be expressed by the reflection impedance matrix $\mathbf{Z_{ref}}$. Thanks to the consistency of thin PCB coil and circuit parameters, we can assume the mutual inductance between the transmitters and receivers has same value M_{tr}. Reflection impedance matrix can be simplified into:

$$\begin{aligned}\mathbf{Z_{ref}} &= \omega^2\mathbf{M_{tr}}^{\mathrm{T}}(\mathbf{Z_{R,new}})^{-1}\mathbf{M_{tr}} \\ &= \frac{m\cdot\omega^2 {M_{\mathrm{tr}}}^2}{Z_{\mathrm{R,new}}} \begin{bmatrix} 1 & 1 & \cdots & 1 \\ 1 & 1 & 1 & \vdots \\ \vdots & 1 & \ddots & 1 \\ 1 & \cdots & 1 & 1 \end{bmatrix}_{n\times n} .\end{aligned} \tag{10}$$

Then, the reflected impedance on $\#i$ transmitting coil is:

$$Z_{\mathrm{ref,i}}=\frac{mn\cdot\omega^2{M_{\mathrm{tr}}}^2}{Z_{\mathrm{R,new}}}. \tag{11}$$

And the total transfer power P_{ref} is equal to:

$$P_{\mathrm{ref}}=\frac{I_{\mathrm{tx}}^2}{2}\mathrm{Re}\left(\frac{mn^2\cdot\omega^2 M_{\mathrm{tr}}^2}{Z_{\mathrm{R,new}}}\right)=mn^2P_{\mathrm{unit}}. \tag{12}$$

where P_{unit} means the unit transfer power which is only related to coupling condition, system load and coil current. Thus, total transfer power P_{ref} has linear relationship with RxUM number m and square-fold relationship with TxUM number n.

C. Influence of Modules Connection Method

In order to ensure balance of the load parameters and bus voltage on each module, all modules will be connected in an array-symmetrical arrangement, as shown in Fig.6. In the figure, n and m with different subscripts (row and col) represent the serial and parallel number of transmitting and receiving modules.

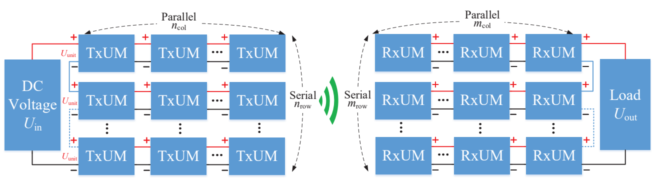

Fig. 6. Diagram of UM connection method.

Suppose the WPT system output requirements are U_{out} and P_{out}; the impedance gain of each rectifier is $\mathrm{G}_{\mathrm{rec}}$. Then, the input resistance of each rectifier is equal to:

$$R_{\mathrm{rec,i}}=\mathrm{G}_{\mathrm{rec}}\frac{m_{\mathrm{col}}}{m_{\mathrm{row}}}\frac{{U_{\mathrm{out}}}^2}{P_{\mathrm{out}}}. \tag{13}$$

Suppose a fully resonance condition is achieved considering the cross-coupling through (7), the reflected impedance $Z_{\mathrm{ref,i}}$ in (11) will be pure resistive and can be calculated by output and coupling conditions:

$$Z_{\mathrm{ref,i}}=R_{\mathrm{ref,i}}=\frac{mn\cdot\omega^2M_{\mathrm{tr}}^2}{\mathrm{G}_{\mathrm{rec}}\frac{m_{\mathrm{col}}}{m_{\mathrm{row}}}\frac{U_{\mathrm{out}}^2}{P_{\mathrm{out}}}+r_{\mathrm{rx}}} \tag{14}$$

Thus, the coupling coil efficiency in modularized and reconfigurable WPT system can be calculated as follow:

$$\eta_{\mathrm{coil}}=\frac{R_{\mathrm{ref}}}{R_{\mathrm{ref}}+r_{\mathrm{tx}}}\frac{R_{\mathrm{rec}}}{R_{\mathrm{rec}}+r_{\mathrm{rx}}} \tag{15}$$

Note the value of r_{rx} and r_{tx} need to consider proximity effect between the stack coils and is function of the module number ($r_{\mathrm{rx}}=f\left(m\right),\ r_{\mathrm{tx}}=f\left(n\right)$), which will have detailed analysis in future research.

Through the design of matching network, the current in transmitting coil I_{tx} will have a relationship $\mathrm{G}_{\mathrm{inv}}$ with the unit DC voltage U_{unit}. Then, the output/input voltage ratio can be calculated based on power balance:

$$\frac{U_{\mathrm{out}}}{U_{\mathrm{in}}}=\frac{\omega M_{\mathrm{tr}}m_{\mathrm{row}}n_{\mathrm{col}}\sqrt{\eta_{\mathrm{rec}}}\mathrm{G}_{\mathrm{inv}}}{\sqrt{2}\sqrt{\mathrm{G}_{\mathrm{rec}}}} \tag{16}$$

It is obvious that there are different UM combination methods which can meet the system requirements. Thus, choosing of UM combination method becomes an optimization problem as shown in (17). The design targets are: Maximize the coil efficiency considering the coils proximity effect; Minimize the using UMs to reduce the cost. The input/output voltage requirements also need to be satisfied as shown in the first constraint. Meanwhile, the combination also needs to consider each UMs' voltage limit and power limit in order to protect the circuit. Therefore, based on above consideration, the wireless power transfer system can be designed flexibly and efficiently in different application scenarios.

$$\begin{aligned}
&\mathrm{OBJ1}:\max\eta_{\mathrm{coil}}\\
&\mathrm{OBJ2}:\min m+n\\
&\mathrm{s.t.}\quad 0.9<\left|\frac{\omega M_{\mathrm{tr}}m_{\mathrm{row}}n_{\mathrm{col}}\sqrt{\eta_{\mathrm{rec}}}\mathrm{G}_{\mathrm{inv}}}{\sqrt{2}\sqrt{\mathrm{G}_{\mathrm{rec}}}}-\frac{U_{\mathrm{out}}}{U_{\mathrm{in}}}\right|<1.1\\
&\qquad n_{\mathrm{row}}\geq\frac{U_{\mathrm{in}}}{U_{\mathrm{unit,max}}},\ m_{\mathrm{row}}\geq\frac{U_{\mathrm{out}}}{U_{\mathrm{unit,max}}}\\
&\qquad n\geq\frac{P_{\mathrm{out}}}{\eta_{\mathrm{sys}}P_{\mathrm{unit,max}}},\ m\geq\frac{P_{\mathrm{out}}}{P_{\mathrm{unit,max}}}
\end{aligned} \tag{17}$$

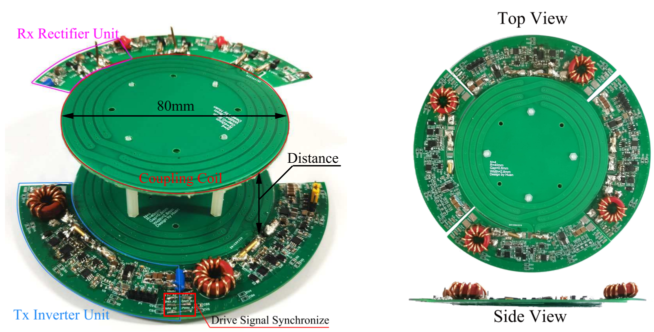

(a) (b)

Fig. 7. Experimental setup (a) System assembly (b) Transmitter with four TxUMs.

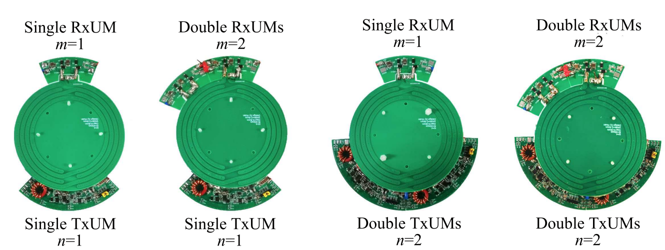

Fig. 8. WPT System with four different modularized combinations.

IV. Experiments Results

The system assembly is shown in Fig. 7(a), the coils in TxUM and RxUM are exactly the same, and their diameter are 80 mm. The thickness of PCB coil (δ) in each UM is equal to 0.4 mm. In the test, transfer distance will vary from 30 mm to 50 mm in order to verify the spatial scalability of the modularized system. Since each TxUM inverter is designed

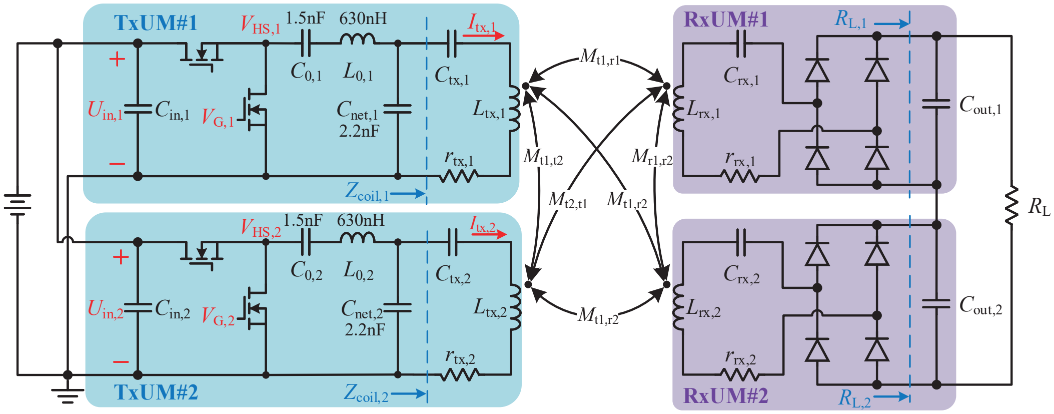

Fig. 9. Circuit schematic of double TxUMs & double RxUMs WPT system

to be a quarter of circle, the WPT transmitter will be put together into a complete circle when using four TxUMs, as shown in Fig.7(b).

In this paper, we mainly test four possible combinations, as shown in Fig. 8, to verified the modularized design concept introduced in Section III. And the circuit schematic of double TxUMs and double RxUMs modularized WPT system is shown in Fig. 9 as an example to illustrate the specific system configuration. Full-bridge rectifier is used in RxUM, which makes $\mathrm{G_{rec}}$ is around 0.81. And equivalent load for each receiver $R_{L,i}$ is equal to 10 Ω. In TxUMs, dc input voltage of each TxUM ($U_{\mathrm{in,i}}$) is equal to 15 V. And combination of half-bridge inverter and classical LCC network (characteristic impedance $Z_{\mathrm{net}} = 10.67\ \Omega$) is used to drive a relative constant transmitting coil current ($I_{\mathrm{tx,i}} = 0.9$ A peak). Thus, $\mathrm{G_{inv}}$ is equal to 0.06. DFLS130 is used as the rectifying diode. Si MOSFET FDMC8032L is chosen as the PA switch, and is driven by LMG1210.

TABLE I
Coil Parameters And Resonance Capacitor.

Single TxUM			Double TxUMs		
L_{tx}	C_{tx}	r_{tx}	$L_{\mathrm{tx,i}}$	$C_{\mathrm{tx,i}}$	$r_{\mathrm{tx,i}}$
1.61 μH	360 pF	0.24 Ω	1.68 μH	176 pF	0.32 Ω
Single RxUM			**Double RxUMs**		
L_{rx}	C_{rx}	r_{rx}	$L_{\mathrm{rx,i}}$	$C_{\mathrm{rx,i}}$	$r_{\mathrm{rx,i}}$
1.60 μH	348 pF	0.23 Ω	1.70 μH	170 pF	0.34 Ω
Three TxUMs (Maxwell Simulation)					
$L_{\mathrm{tx,1}}$	$L_{\mathrm{tx,2}}$	$L_{\mathrm{tx,3}}$	$r_{\mathrm{tx,1}}$	$r_{\mathrm{tx,2}}$	$r_{\mathrm{tx,3}}$
1.74 μH	1.73 μH	1.73 μH	0.61 Ω	0.78 Ω	0.62 Ω

Coil parameters in different modularized combinations are shown in Table I. Compared with the single UM, double UMs structure has larger self-inductance and inner resistance. The existence of cross-coupling ($M_{\mathrm{t1,t2}}, M_{\mathrm{r1,r2}}$) in double UMs structure leads to smaller resonance capacitor according to (7). Another big issue in this modularized structure is the proximity effect among the PCB coils. Fig. 10 shows the inner-turn's current density simulation results of modularized coils based on MAXWELL. The results show that inner resistance of each coil will increase with UM using number. Meanwhile, asymmetric combination of modularized coils, e.g. three TxUMs structure, will lead to a larger resistance in the middle UM because of the proximity effect. Meanwhile, using more TxUMs will increase the reflected impedance according to (11). Thus, the increase of coil resistance caused by additional TxUMs will not significantly influence coil efficiency and it maybe an important concerns in the optimization of modularized WPT system. Because of actual layout requirements, the number of UMs is also limited ($m, n \leqslant 4$), which means $r_{\mathrm{tx,i}}$ of middle UMs will not deviate too much from the one of outer UMs, as shown in Fig.10(c). Thus, the system can still maintain balance power distribution among UMs when $R_{\mathrm{ref,i}}$ and $R_{\mathrm{rec,i}}$ are designed relative large.

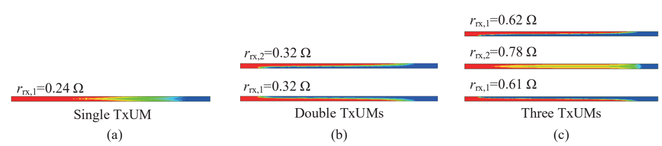

Fig. 10. MAXWELL simulation of proximity effect in modularized design. (a) Single TxUm (b) Double TxUMs (c) Three TxUMs.

The tested mutual inductance and corresponding unit power (P_{unit}) are shown in Fig.11(a). In the actual module design, each UM has certain thickness δ, which makes the coupling among TxUMs and RxUMs have tiny difference. To describe this difference, we define a ratio:

$$M_{\mathrm{tr}}\mathrm{Ratio} = \frac{\max\left(M_{\mathrm{ti,rj}}\right)}{\min\left(M_{\mathrm{ti,rj}}\right)}. \tag{18}$$

According to Fig.11(b), $M_{\mathrm{tr}}\mathrm{Ratio}$ will increase significantly with the PCB coil thickness. This coupling divergence will also lead to power unbalance among the modules, as shown in Fig.11(c). Thus, to maintain power balance in each module, longer transfer distance and thinner PCB of coupling coils are

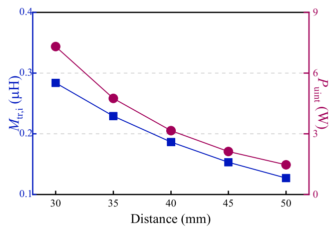

(a)

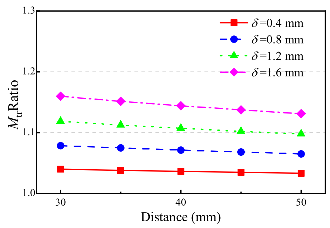

(b)

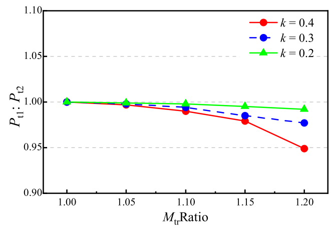

(c)

Fig. 11. (a) $M_{\mathrm{tr,i}}$ vs. Distance. (b) $M_{\mathrm{tr}}\mathrm{Ratio}$ vs. Distance. (c) Power ratio in TxUM1 and TxUM2 vs. $M_{\mathrm{tr}}\mathrm{Ratio}$

preferred in modularized system design. Note choosing coil thickness also needs to consider the proximity effect, which will achieve overall optimization in future research.

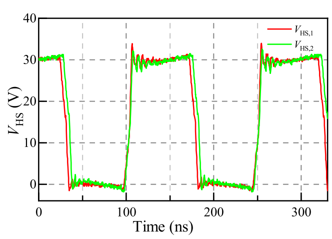

(a)

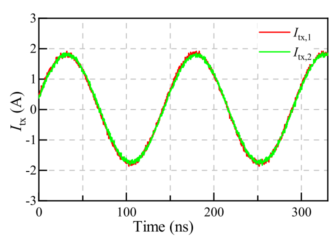

(b)

Fig. 12. Waveform in TxUMs (a) V_{HS}. (b) I_{tx}

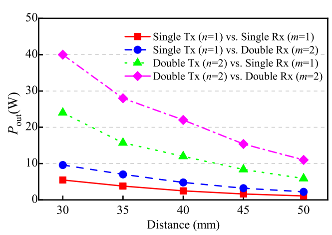

(a)

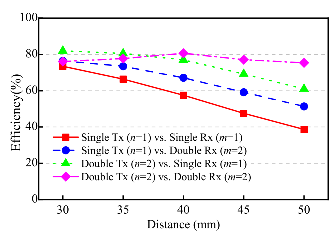

(b)

Fig. 13. Experiment results of power and efficiency versus transfer distance.(a)P_{out}. (b)η_{sys}

Fig. 12 compares the consistency of synchronous drive signals of the double TxUMs (the waveforms of AC output voltage V_{HS} and the coil current I_{tx} in the half-bridge topology). In the experiments, the output power and dc-dc efficiency (considering the power loss in all UMs and coupling coils) are measured under different transfer distance, as shown in Fig. 13. The results show that transfer power will increase with the UM number, as shown in Fig.13(a). Considering the calculated unit power (red line in Fig. 11(a)), the transfer power in WPT system with different number of UMs satisfies the equation (12) quite well in all distance condition. Based on this experiment results, when WPT system requires longer transfer distance or higher power output, the system can simply increase the number of modules to meet the power output in different transfer distance. Meanwhile, the transmission efficiency will achieve obvious improvement with additional UMs in Fig.13(b), especially in large transfer distance condition. Therefore, the above experimental results basically prove the feasibility of the proposed modularized and reconfigurable WPT design concept.

V. Conclusion

In this article, three different kinds of WPT architectures are analyzed and compared first. Base on that, the combination of MHz operation frequency and the function modules architecture is chosen as the basic system architecture. Then, mathematic derivation of this architecture is shown in detailed. Based on that, this paper proposes a basic design concept for modularized and reconfigurable WPT system which will shorten the design period and decrease the cost in different WPT application. Finally, the influence of proximity effect and mutual inductance divergence achieve briefly analysis according to simulation and test. And the modularized design concept is basically verified by the power and efficiency test results of four different combinations of UMs. Future research will focus on the optimal design of module coils considering the proximity effect, and optimized UMs combination method based on system input/output requirements.

References

[1] S. Y. R. Hui, W. Zhong, and C. K. Lee, “A critical review of recent progress in mid-range wireless power transfer,” *IEEE Trans. Power Electron.*, vol. 29, no. 9, pp. 4500–4511, Sep. 2014.

[2] M. Pinuela, D. C. Yates, S. Lucyszyn, and P. D. Mitcheson, “Maximizing dc-to-load efficiency for inductive power transfer,” *IEEE Trans. Power Electron.*, vol. 28, no. 5, pp. 2437–2447, May 2013.

[3] S. Aldhaher, D. C. Yates, and P. D. Mitcheson, “Design and development of a class EF_2 inverter and rectifier for multimegahertz wireless power transfer systems,” *IEEE Trans. Power Electron.*, vol. 31, no. 12, pp. 8138–8150, Dec. 2016.

[4] J. Choi, D. Tsukiyama, and J. Rivas, “Comparison of sic and egan devices in a 6.78 mhz 2.2 kw resonant inverter for wireless power transfer,” in *2016 IEEE Energy Conversion Congress and Exposition (ECCE)*, 2016, pp. 1–6.

[5] Q. Deng, P. Sun, W. Hu, D. Czarkowski, M. K. Kazimierczuk, and H. Zhou, “Modular parallel multi-inverter system for high-power inductive power transfer,” *IEEE Transactions on Power Electronics*, vol. 34, no. 10, pp. 9422–9434, 2019.

[6] H. Zhou, J. Chen, Q. Deng, F. Chen, A. Zhu, W. Hu, and X. Gao, “Input-series output-equivalent-parallel multi-inverter system for high-voltage and high-power wireless power transfer,” *IEEE Transactions on Power Electronics*, vol. 36, no. 1, pp. 228–238, 2021.